ACS Photonics

pubs.acs.org/journal/apchd5 Letter

Inverse Design of Optical Vortex Beam Emitters

Alexander D. White,* Logan Su, Daniel I. Shahar, Ki Youl Yang, Geun Ho Ahn, Jinhie L. Skarda, Siddharth Ramachandran, and Jelena Vučković*

Cite This: https://doi.org/10.1021/acsphotonics.2c01007 Read Online

ACCESS | Metrics & More | Article Recommendations | Supporting Information

ABSTRACT: Vortex beams are stable solutions of Maxwell's equations that carry phase singularities and orbital angular momentum, unique properties that give rise to many applications in the basic sciences, optical communications, and quantum technologies. Scalable integration and fabrication of vortex beam emitters will allow these applications to flourish and enable new applications that are not possible with traditional optics. Here we present a general framework to generate integrated vortex beam emitters using photonic inverse design. We experimentally demonstrate the generation of vortex beams with angular momentum spanning $-3\hbar$ to $3\hbar$. We show the generality of this design procedure by designing a vortex beam multiplexer capable of exciting a custom vortex beam fiber. Finally, we produce foundry-fabricated beam emitters with wide bandwidths and high efficiencies that take advantage of multilayer heterogeneous integration.

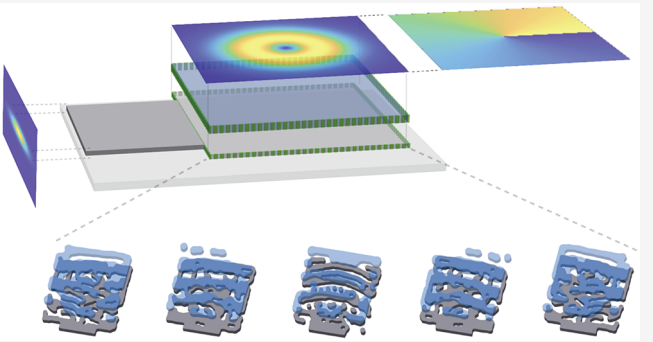

KEYWORDS: *inverse design, integrated photonics, OAM, optical vortexes, mode multiplexing, heterogeneous integration*

INTRODUCTION

Optical vortex beams and the orbital angular momentum (OAM) they carry are useful in a vast array of applications, including classical and quantum communication, super-resolution microscopy, optical trapping and manipulation, and metrology.[1−5] For example, OAM can be used as an additional entanglement basis in flying qubits[3,6] or as an additional basis for data encoding in ultrahigh-bandwidth communication.[4] While these beams are traditionally generated by phase plates or spatial light modulators, efforts have been made to integrate optical vortex beam emitters onto nanophotonic platforms. Such integration allows for the construction of extremely compact vortex beam generators in platforms that can provide additional functionality and optical processing.

Initial demonstrations of on-chip vortex beam generators consisted of ring resonators with gratings whose periodicity mismatch with the optical mode enforced the radial phase required for an OAM beam.[7] While this design is capable of producing high-quality OAM beams in a compact area, the resonant nature of the devices limits their bandwidth and prevents multiplexing. Since then, many strategies for on-chip vortex beam generation have been demonstrated, including OAM lasers,[8−11] metasurfaces,[12−14] and analytical[15−17] and computational[18−20] grating design.

Here we provide a general framework for the design of integrated vortex beam emitters using adjoint optimized photonics inverse design. We first demonstrate OAM beam generation of $l = -3$ to 3 in single-layer silicon photonics. We then show a three-mode OAM multiplexer designed to launch modes into a custom $l = -1, 0, 1$ fiber. Finally, we utilize the well-controlled fabrication and heterogeneous integration of a commercial foundry (A*STAR, AMF) to demonstrate high-fidelity, wide-bandwidth, and efficient vortex beam emitters. While we focus on vortex beam generation here, the same inverse design protocol can be used to optimize beam emitters and multiplexers for arbitrary free-space modes.

INVERSE DESIGN FRAMEWORK

Vortex beams consist of a Laguerre−Gaussian field profile with a phase that is linearly proportional to the angle and integrates to 2π times an integer l, the orbital angular momentum:

$$E_{p,l}(r,\phi) = \frac{1}{w_0} L_p^{|l|}\left(\frac{2r^2}{{w_0}^2}\right)\sqrt{\frac{2p!}{\pi(p+|l|)!}}\left(\frac{r\sqrt{2}}{w_0}\right)^{|l|} e^{-r^2/{w_0}^2} e^{il\phi} \quad (1)$$

Special Issue: Optimized Photonics and Inverse Design

Received: June 29, 2022

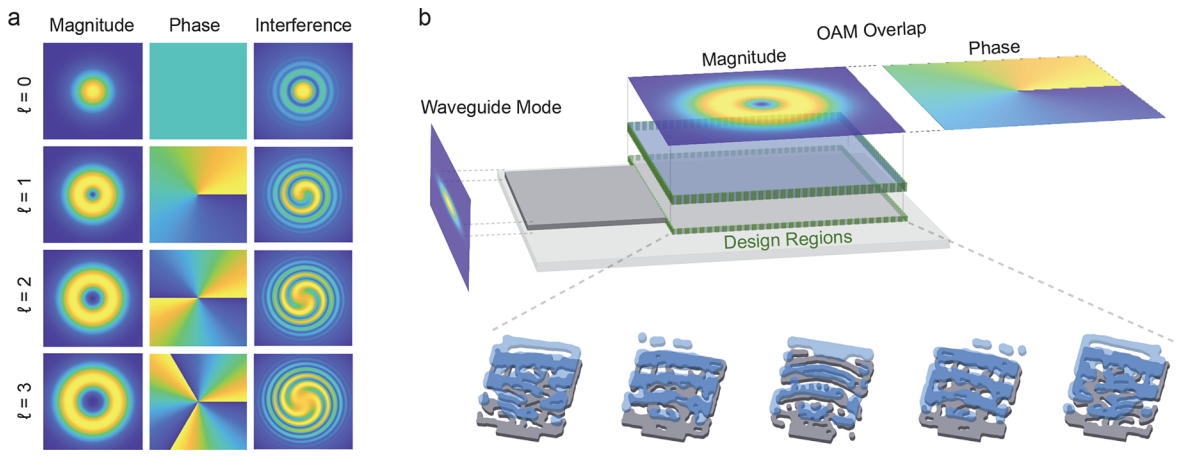

Figure 1. Inverse Design Approach. (a) Cross-section of vortex beams with OAM *l* from 0 to 3. Plots show the magnitude, the phase, and the interference pattern generated by interference with a Gaussian beam. (b) Schematic of the inverse design approach to generate optical vortex beam emitters. We optimize an area (denoted by design regions) that takes a waveguide mode as input and generates a field pattern that has a maximum overlap with the desired OAM beam. Gray layers show silicon, and blue layers show silicon nitride.

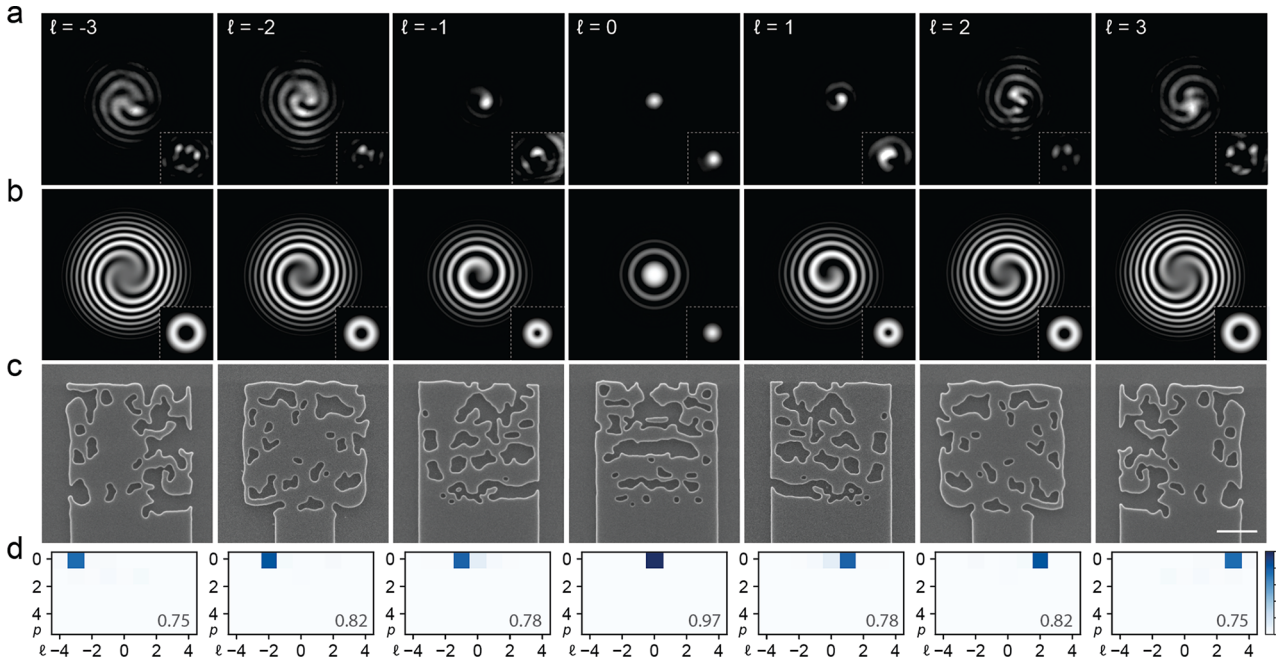

Figure 2. Single layer vortex beam emitters. (a) Measured interference patterns generated from single-layer silicon OAM gratings driven with a 1515 nm laser through the waveguide and a colinear Gaussian beam. The insets show the corresponding measured intensity patterns. (b) Ideal interference patterns and (insets) beam intensities corresponding to the patterns in (a). (c) SEM images of the vortex beam emitter devices used in (a). The scale bar is 1 μm. (d) Simulated mode decomposition into LG-OAM modes; *p* gives the radial order, *l* gives the angular momentum order, and text gives the mode purity.

where p is the radial index and w_0 is the beam waist. For first-order radial modes, the simplest OAM beams, this profile simplifies to

$$E_l(r, \phi) = \frac{1}{w_0}\sqrt{\frac{1}{\pi |l|!}}\left(\frac{r\sqrt{2}}{w_0}\right)^{|l|} e^{-r^2/w_0^2} e^{il\phi} \tag{2}$$

examples of which are shown in Figure 1a. Vortex beams can have nearly arbitrary polarization, including topologically interesting spatially varying polarization coupled with the beam shape,[21] but here we use spatially homogeneous linear polarization for simplicity.

To design arbitrary beam emitters, we optimize a structure that takes a waveguide mode as input and launches a beam out of the plane of the chip whose electric field overlaps maximally with the desired beam shape in free space (Figure 1b). To efficiently optimize the structure, we use an adjoint optimization approach that allows us to calculate the optimization gradients at every point with only two simulations.[22,23] Using this optimization procedure, we maximize the overlap of the field lauched by the device and the desired spatial mode pattern:

$$\max_{\varepsilon} |\mathbf{c}^{\dagger}\mathbf{x}(\varepsilon)|^2$$

where $\mathbf{x}(\varepsilon)$ is the vectorized electric field due to the designed-permitted distribution and $\mathbf{c}$ is the vectorized electric field of the desired OAM beam in free space. Here we optimize the

https://doi.org/10.1021/acsphotonics.2c01007
ACS Photonics XXXX, XXX, XXX−XXX

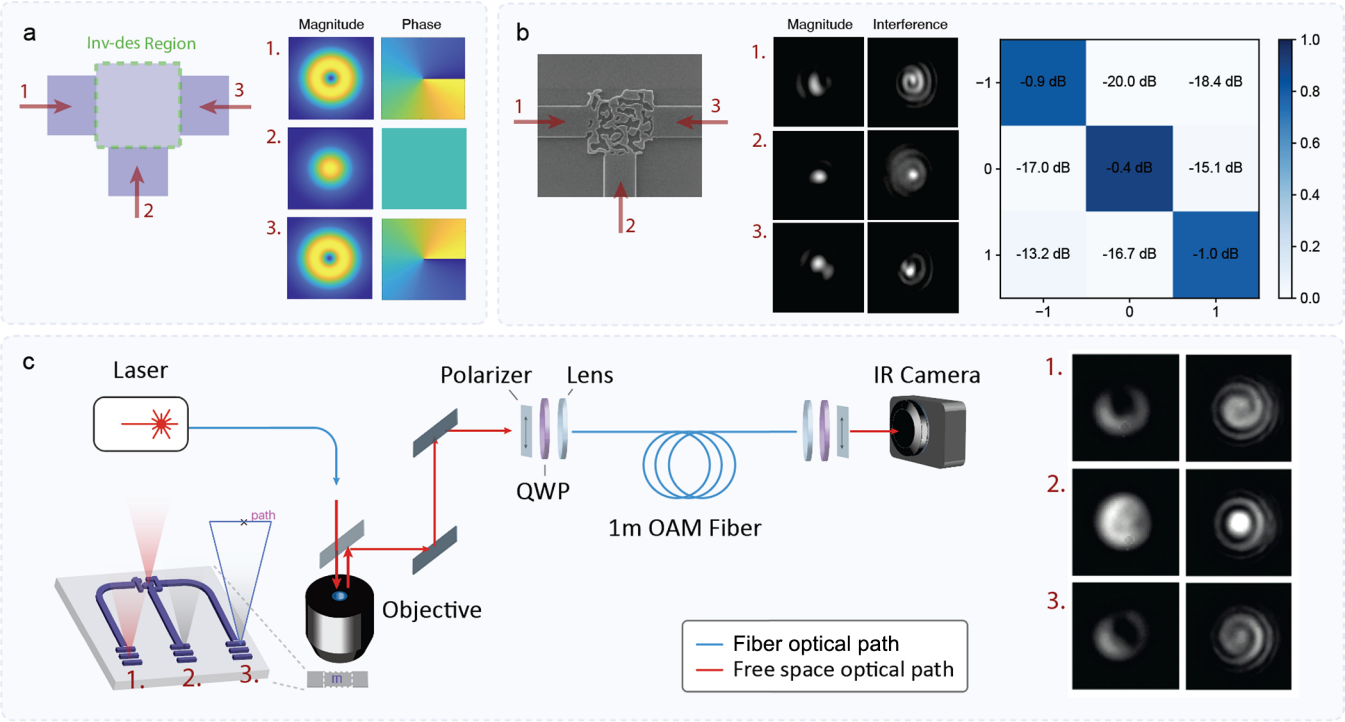

Figure 3. Vortex beam multiplexer. (a) Schematic of the vortex beam multiplexer design. The inverse design region has three waveguide inputs and is optimized to launch $l = -1$, 0, 1 from ports 1, 2, and 3, respectively. In order to efficiently multiplex these beams, all are designed to emit light that is linearly polarized along the y (vertical) axis. (b) SEM and measured intensity and interference patterns from the fabricated device, measured at 1510 nm. The heat plot shows the simulated crosstalk between the modes. (c) Schematic of the fiber coupling measurement and the measured patterns. The chip is excited by a laser through one of three input ports. The resulting y-polarized output of the chip is sent through the OAM fiber and finally imaged on an IR camera.

emitters to form vortex beams, but this design approach is general and can be applied to any desired spatial field pattern.

RESULTS

We first optimize compact devices that emit vortex beams for $l = -3$ to 3. These devices are 3 μm × 3 μm and fabricated using electron beam lithography on an air-clad 220 nm silicon-on-insulator platform. They operate in the telecom band and are designed with an 80 nm minimum feature size. To measure the emission properties, we excite an on-chip waveguide coupled to a device and collect the emitted light through a high-NA objective. We then interfere the beam from the device with a Gaussian beam generated from the same laser source and image the resulting intensity pattern. Figure 2 shows the theoretical interference patterns from ideal vortex beams as well as the measured interference patterns (with simulations shown in Figure S2). The spiral pattern is formed by the combination of a curved phase front radially and the angular OAM phase; the direction of spiraling shows the sign of the OAM, and the number of teeth shows the OAM order.

To demonstrate the generality of this design approach, we optimize a device to launch multiplexed $l = -1$, 0, 1 modes into a custom OAM-supporting optical fiber.[24,25] Such multiplexing normally requires free-space optics or custom 3D devices.[26] The device is designed to launch an $l = -1$ mode when excited from the left waveguide, $l = 1$ when excited from the right waveguide, and $l = 0$ when excited from the bottom waveguide (Figure 3a). Additionally, all of these modes are designed to be y-polarized so that a polarizer can be used to filter out undesired mode coupling in the fiber. This leads to the additional design complication that the $l = 0$ mode must be launched with the orthogonal polarization to its input waveguide mode. Even with these additional constraints, the optimization procedure yielded a compact 3 μm × 3 μm device that was able to generate all three modes with a simulated maximum crosstalk of −13.2 dB and an average crosstalk of −16.7 dB (Figures 3b and S3). To launch these modes into a custom OAM fiber, we pass the output fields through a polarizer and quarter-wave plate to match the circularly polarized eigenmodes of the fiber and use a lens to focus the collimated beams on the fiber core. To image the fiber modes with a camera, we employ another lens, quarter-wave plate, and polarization beamsplitter (Figure 3c). This leads to beams that are even more pure than those directly from the multiplexer, as the fiber filters out any higher-order modes from design nonidealities and scattering.

Finally, we utilize the well-controlled fabrication and heterogeneous integration from the A*STAR AMF foundry to generate high-fidelity, wide-bandwidth, and efficient vortex beam emitters. To do this, we implement an FDFD adjoint optimization package capable of the simultaneous optimization of multiple design regions.[22] In combination with multilayer photonics processing,[27] this allows us to design fully 3D structures parametrized by slices in the z dimension. We design $l = -2$ to 2 devices consisting of two co-optimized layers: a 220 nm silicon layer with a 140 nm minimum feature size and a 400 nm silicon nitride layer with a 300 nm minimum feature size. The layers are separated by 250 nm and are clad with silicon oxide.

The measured intensity and interference patterns of these devices are shown in Figure 4a (simulated results are shown in Figures S4−S6). The additional degrees of freedom given by

https://doi.org/10.1021/acsphotonics.2c01007
ACS Photonics XXXX, XXX, XXX−XXX

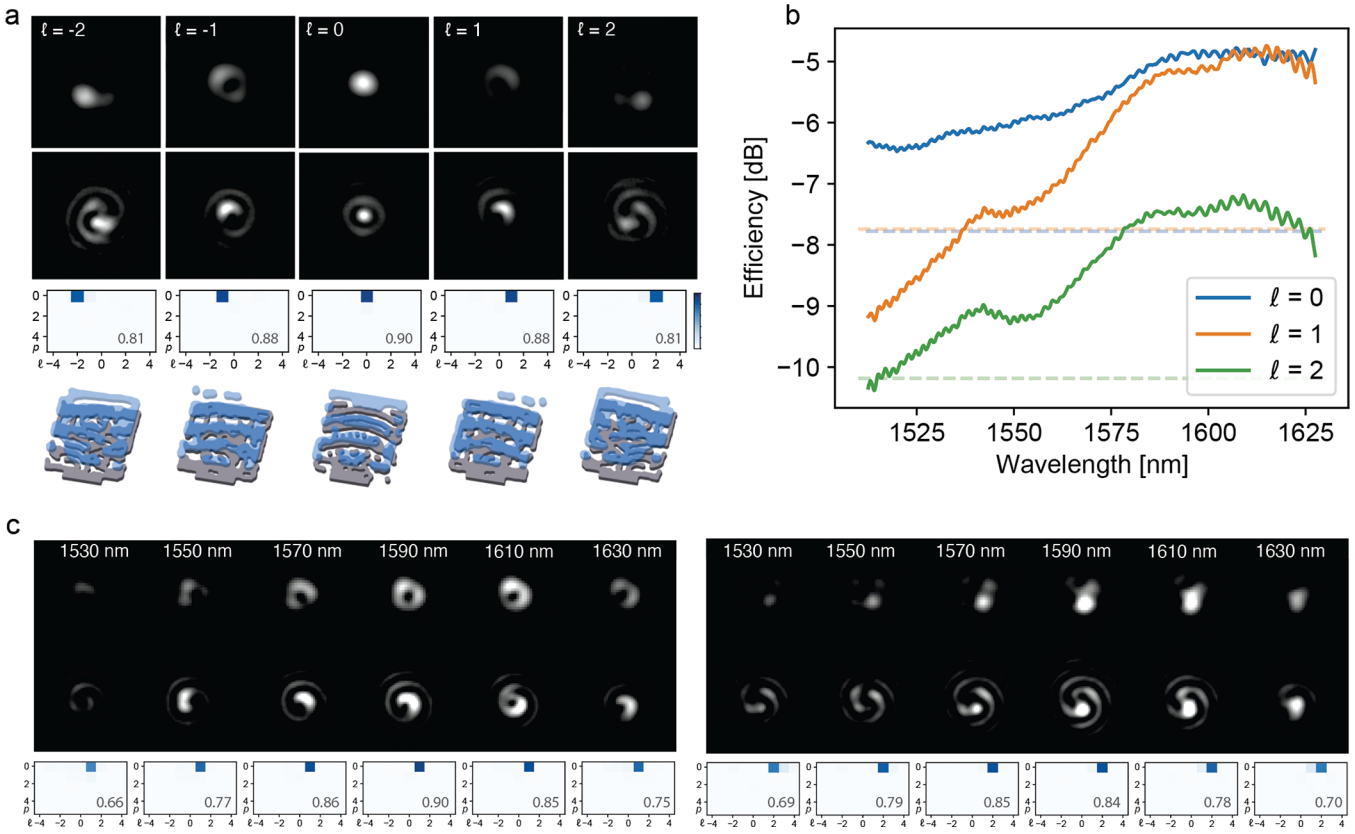

Figure 4. Foundry-fabricated two-layer beam emitters. (a) Intensity (top row) and interference (second row) patterns from foundry-fabricated two-layer beam emitters measured at 1570 nm. The third row shows the simulated LG-OAM decompositions and mode purities. The bottom row shows 3D representations of the grating devices, with silicon in gray and silicon nitride in blue. (b) Efficiencies of gratings measured using a 50 μm core multimode fiber. The $l = -1, -2$ efficiencies are identical to the $l = 1, 2$ efficiencies, as the devices are mirror images of each other. Dashed lines show 3 dB from each maximum. (c) Wavelength sweep of $l = 1$ and $l = 2$ intensity and interference patterns and mode decompositions from 1530 to 1630 nm.

the two-layer design and the better-controlled fabrication process of the foundry allow us to see significant improvements in the beam shapes. Additionally, these emitters are able to maintain OAM emission across at least a 100 nm optical bandwidth (Figure 4b). To measure the emitter efficiency, we couple to a multimode fiber that supports OAM beams and sweep the input wavelength, and we find that the 3 dB bandwidths exceed 100 nm (Figure 4c).

CONCLUSION

We have demonstrated a general optimization technique for beam emitters and applied it to generate optical vortex beams. We have shown compact generation of $l = -3$ to 3 vortex beams, a vortex beam multiplexer, and high-performance foundry-fabricated heterogeneously integrated multilayer devices. The robustness of this approach in generating multiple orders and combinations of vortex beams and its ability to translate to foundry processing open the door for applications in classical and quantum communications, information processing, and imaging.

ASSOCIATED CONTENT

Data Availability Statement

Code to inverse design these devices using goos is publicly available at https://github.com/alex-d-white/OAM_Invese_Design.

Supporting Information

The Supporting Information is available free of charge at https://pubs.acs.org/doi/10.1021/acsphotonics.2c01007.

Optimization methods, detailed experimental setup, and simulated field patterns (PDF)

AUTHOR INFORMATION

Corresponding Authors

Alexander D. White − *E. L. Ginzton Laboratory, Stanford University, Stanford, California 94305, United States;* orcid.org/0000-0002-5387-310X; Email: adwhite@stanford.edu

Jelena Vučković − *E. L. Ginzton Laboratory, Stanford University, Stanford, California 94305, United States;* Email: jela@stanford.edu

Authors

Logan Su − *E. L. Ginzton Laboratory, Stanford University, Stanford, California 94305, United States*

Daniel I. Shahar − *Department of Electrical and Computer Engineering, Boston University, Boston, Massachusetts 02215, United States*

Ki Youl Yang − *E. L. Ginzton Laboratory, Stanford University, Stanford, California 94305, United States;* orcid.org/0000-0002-0587-3201

https://doi.org/10.1021/acsphotonics.2c01007
ACS Photonics XXXX, XXX, XXX−XXX

Geun Ho Ahn − *E. L. Ginzton Laboratory, Stanford University, Stanford, California 94305, United States;* orcid.org/0000-0002-4761-7804

Jinhie L. Skarda − *E. L. Ginzton Laboratory, Stanford University, Stanford, California 94305, United States;* orcid.org/0000-0003-0785-4984

Siddharth Ramachandran − *Department of Electrical and Computer Engineering, Boston University, Boston, Massachusetts 02215, United States*

Complete contact information is available at: https://pubs.acs.org/10.1021/acsphotonics.2c01007

Notes

The authors declare no competing financial interest.

■ ACKNOWLEDGMENTS

The authors thank Kasper Van Gasse and Rahul Trivedi for productive discussions and Mohamad Idjadi and Firooz Aflatouni for assistance in foundry integration. This research was supported by the Air Force Office of Scientific Research (FA9550-17-1-0002), DARPA under the PIPES Program, the Vannevar Bush Faculty Fellowship (N00014-19-1-2632), and ONR-MURI (N00014-20-1-2450).

■ REFERENCES

(1) Ni, J.; Huang, C.; Zhou, L.-M.; Gu, M.; Song, Q.; Kivshar, Y.; Qiu, C.-W. Multidimensional phase singularities in nanophotonics. *Science* **2021**, *374*, No. eabj0039.

(2) Shen, Y.; Wang, X.; Xie, Z.; Min, C.; Fu, X.; Liu, Q.; Gong, M.; Yuan, X. Optical vortices 30 years on: OAM manipulation from topological charge to multiple singularities. *Light: Sci. Appl.* **2019**, *8*, 90.

(3) Barreiro, J. T.; Wei, T.-C.; Kwiat, P. G. Beating the channel capacity limit for linear photonic superdense coding. *Nat. Phys.* **2008**, *4*, 282−286.

(4) Wang, J.; Yang, J.-Y.; Fazal, I. M.; Ahmed, N.; Yan, Y.; Huang, H.; Ren, Y.; Yue, Y.; Dolinar, S.; Tur, M.; et al. Terabit free-space data transmission employing orbital angular momentum multiplexing. *Nat. Photonics* **2012**, *6*, 488−496.

(5) Ren, H.; Li, X.; Zhang, Q.; Gu, M. On-chip noninterference angular momentum multiplexing of broadband light. *Science* **2016**, *352*, 805−809.

(6) Otte, E.; Rosales-Guzmán, C.; Ndagano, B.; Denz, C.; Forbes, A. Entanglement beating in free space through spin−orbit coupling. *Light: Sci. Appl.* **2018**, *7*, 18009−18009.

(7) Cai, X.; Wang, J.; Strain, M. J.; Johnson-Morris, B.; Zhu, J.; Sorel, M.; O'Brien, J. L.; Thompson, M. G.; Yu, S. Integrated compact optical vortex beam emitters. *Science* **2012**, *338*, 363−366.

(8) Miao, P.; Zhang, Z.; Sun, J.; Walasik, W.; Longhi, S.; Litchinitser, N. M.; Feng, L. Orbital angular momentum microlaser. *Science* **2016**, *353*, 464−467.

(9) Liu, Q.; Zhao, Y.; Ding, M.; Yao, W.; Fan, X.; Shen, D. Wavelength-and OAM-tunable vortex laser with a reflective volume Bragg grating. *Opt. Express* **2017**, *25*, 23312−23319.

(10) Kitamura, K.; Kitazawa, M.; Noda, S. Generation of optical vortex beam by surface-processed photonic-crystal surface-emitting lasers. *Opt. Express* **2019**, *27*, 1045−1050.

(11) Bahari, B.; Hsu, L.; Pan, S. H.; Preece, D.; Ndao, A.; El Amili, A.; Fainman, Y.; Kanté, B. Photonic quantum Hall effect and multiplexed light sources of large orbital angular momenta. *Nat. Phys.* **2021**, *17*, 700−703.

(12) Yu, N.; Genevet, P.; Kats, M. A.; Aieta, F.; Tetienne, J.-P.; Capasso, F.; Gaburro, Z. Light propagation with phase discontinuities: generalized laws of reflection and refraction. *Science* **2011**, *334*, 333−337.

(13) Chen, M. L.; Jiang, L. J.; Sha, W. E. Orbital angular momentum generation and detection by geometric-phase based metasurfaces. *Appl. Sci.* **2018**, *8*, 362.

(14) Barati Sedeh, H.; Salary, M. M.; Mosallaei, H. Time-varying optical vortices enabled by time-modulated metasurfaces. *Nanophotonics* **2020**, *9*, 2957−2976.

(15) Su, T.; Scott, R. P.; Djordjevic, S. S.; Fontaine, N. K.; Geisler, D. J.; Cai, X.; Yoo, S. Demonstration of free space coherent optical communication using integrated silicon photonic orbital angular momentum devices. *Opt. Express* **2012**, *20*, 9396−9402.

(16) Zhou, N.; Zheng, S.; Cao, X.; Zhao, Y.; Gao, S.; Zhu, Y.; He, M.; Cai, X.; Wang, J. Ultra-compact broadband polarization diversity orbital angular momentum generator with 3.6 × 3.6 μm^2 footprint. *Sci. Adv.* **2019**, *5*, No. eaau9593.

(17) Zhao, Z.; Fan, S. Design principles of apodized grating couplers. *J. Lightwave Technol.* **2020**, *38*, 4435−4446.

(18) Xie, Z.; Lei, T.; Li, F.; Qiu, H.; Zhang, Z.; Wang, H.; Min, C.; Du, L.; Li, Z.; Yuan, X. Ultra-broadband on-chip twisted light emitter for optical communications. *Light: Sci. Appl.* **2018**, *7*, 18001−18001.

(19) Song, H.; Zhao, Z.; Zhang, R.; Song, H.; Zhou, H.; Pang, K.; Du, J.; Li, L.; Liu, C.; Su, X.; et al. Utilizing phase delays of an integrated pixel-array structure to generate orbital-angular-momentum beams with tunable orders and a broad bandwidth. *Opt. Lett.* **2020**, *45*, 4144−4147.

(20) White, A.; Yang, K.; Vučković, J. Inverse-designed Optical Vortex Beam Emitters. In *Conference on Lasers and Electro-Optics*; OSA Technical Digest; Optica Publishing Group, 2021; SM4C-2.

(21) Bauer, T.; Banzer, P.; Karimi, E.; Orlov, S.; Rubano, A.; Marrucci, L.; Santamato, E.; Boyd, R. W.; Leuchs, G. Observation of optical polarization Möbius strips. *Science* **2015**, *347*, 964−966.

(22) *Goos*, 2021. https://github.com/stanfordnqp/spins-b (accessed 2022-09-09).

(23) Su, L.; Vercruysse, D.; Skarda, J.; Sapra, N. V.; Petykiewicz, J. A.; Vučković, J. Nanophotonic inverse design with SPINS: Software architecture and practical considerations. *Appl. Phys. Rev.* **2020**, *7*, 011407.

(24) Bozinovic, N.; Golowich, S.; Kristensen, P.; Ramachandran, S. Control of orbital angular momentum of light with optical fibers. *Opt. Lett.* **2012**, *37*, 2451−2453.

(25) Bozinovic, N.; Yue, Y.; Ren, Y.; Tur, M.; Kristensen, P.; Huang, H.; Willner, A. E.; Ramachandran, S. Terabit-scale orbital angular momentum mode division multiplexing in fibers. *Science* **2013**, *340*, 1545−1548.

(26) Lightman, S.; Bleyhman, I.; Somers, L.; Hurvitz, G.; Gvishi, R.; Rusch, L. A.; Arie, A. Integrated orbital angular momentum mode sorters on vortex fibers. *Opt. Lett.* **2022**, *47*, 3491−3494.

(27) Sacher, W. D.; Huang, Y.; Lo, G.-Q.; Poon, J. K. Multilayer silicon nitride-on-silicon integrated photonic platforms and devices. *J. Lightwave Technol.* **2015**, *33*, 901−910.